Supplementary information

Hyperspectral Remote Sensing for Monitoring Crop Disease: Applications, Challenges, and Perspectives

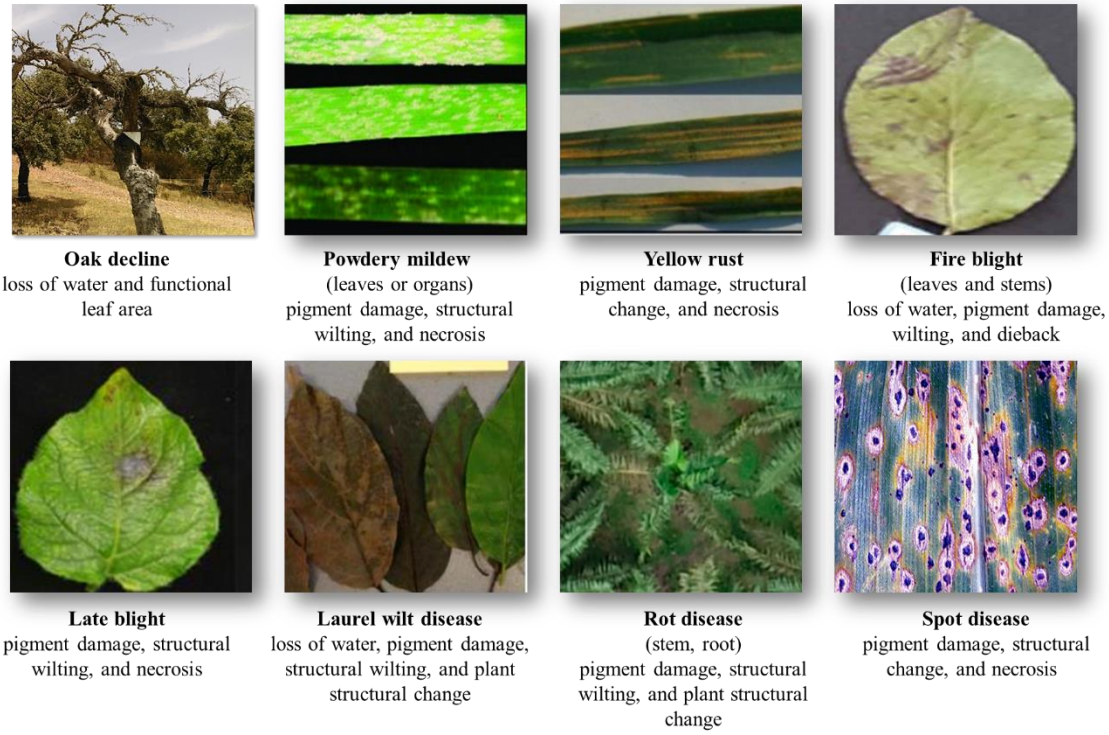

Fig. S2.1. *Examples of plant disease and corresponding affected symptoms. Note: Images were modified from the following papers: Hornero et al. (2021), Huang et al. (2015), Huang et al. (2015), Bagheri et al. (2018), Gold et al. (2020), Abdulridha et al. (2016), Kurihara et al. (2022), and Loladze et al. (2019).*

Table s2.1 Vegetation indices (VIs) for monitoring crop diseases

Name	**Abbr.**	**Equation**	**Pathogen (host)**	**Orig. Ref.**	**Dis. Ref.**
VIs for plant biophysical properties: structure, crop cover					
Normalized difference vegetation index	NDVI	$\frac{R_{800}-R_{670}}{R_{680}+R_{670}}$	Verticillium wilt (olive), bacterial spot (tomato)	(Rouse et al., 1974)	(Abdulridha et al., 2020; Calderon et al., 2013)

Middle-infrared normalized difference	MND	$\frac{R_{1080}-R_{1675}}{R_{1080}+R_{1675}}$	*Phytophthora*-induced disease (oak)	(Malthus et al., 1993)	(Hornero et al., 2021)
Renormalized difference vegetation index	RDVI	$\frac{R_{800}-R_{670}}{\sqrt{R_{800}+R_{670}}}$	Tar spot complex (maize), Fire blight (apple trees)	(Chen, 1996)	(Loladze et al., 2019; Skoneczny et al., 2020)
Modified simple ratio	MSR	$\frac{R_{800}-R_{670}-1}{\sqrt{R_{800}+R_{670}+1}}$	Fire blight (apple trees)	(Chen, 1996)	(Skoneczny et al., 2020)
Modified triangular vegetation index	MTVI	$1.2(1.2(R_{800}-R_{550})-2.5(R_{670}-R_{550}))$	Fire blight (apple trees)	(Haboudane et al., 2004)	(Skoneczny et al., 2020)
VIs for plant biochemical properties: pigments, water, and nitrogen					
Chlorophyll					
Vogelmann index	VOG	$\frac{R_{734}-R_{747}}{R_{715}+R_{726}}$	*Xylella fastidiosa* (olive, almond)	(Vogelmann et al., 1993)	(Camino et al., 2021; Poblete et al., 2020; Zarco-Tejada et al., 2018)
Transformed chlorophyll absorption ratio	TCARI	$3((R_{700}-R_{670})-0.2(R_{700}-R_{550})\frac{R_{700}}{R_{670}})$	*Xylella fastidiosa* (almond), yellow rust (wheat)	(Haboudane et al., 2002a)	(Camino et al., 2021; Devadas et

					al., 2009)
Transformed chlorophyll absorption ratio/optimized soil adjusted vegetation index	TCARI/OSAVI	$\frac{TCARI}{\frac{(1+0.16)(R_{800}-R_{670})}{R_{900}+R_{670}+0.16}}$	*Xylella fastidiosa* (olive)	(Haboudane et al., 2002a)	(Poblete et al., 2020; Zarco-Tejada et al., 2018)
Modified chlorophyll absorption ratio index	MCARI	$\frac{1.2\left[2.5(R_{800}-R_{670})-1.3(R_{800}-R_{550})\right]}{\sqrt{(2R_{800}+1)^2-(6R_{800}-5\sqrt{R_{680}})-0.5}}$	Tar spot complex (maize)	(Haboudane et al., 2004)	(Lolade et al., 2019)
Pigment specific simple ratio, $for\ Chl$a	PSSRa	$\frac{R_{800}}{R_{680}}$	Leaf blast (rice)	(Blackburn, 1998)	(Tian et al., 2021)
Pigment specific normalized difference, $for\ Chl$a	PSNDa	$\frac{R_{800}-R_{675}}{R_{680}+R_{675}}$	Leaf blast (rice)	(Blackburn, 1998)	(Tian et al., 2021)
Chlorophyll green	Chl green	$\frac{R_{760\sim800}}{R_{540\sim560}}$	bacterial spot (tomato), target spot (tomato), downy mildew (watermelon)	(Gitelson et al., 2003)	(Abdulridha et al., 2020; Abdulridha et al., 2022)
Triangular vegetation index	TVI	$0.5[120(R_{761}-R_{581})-200(R_{651}-R_{581})]$	target spot (tomato)	(Broge and Leblanc, 2001)	(Abdulridha et al., 2020)
Carotenoids					
Carotenoid reflectance index	CRI_{700M}	$\frac{1}{R_{510}}-\frac{1}{R_{710}}$	*Xylella fastidiosa* (olive)	(Gitelson et al., 2006; Gitelson et al.,	(Poblete et al., 2020; Zarco-Tejad

				2003)	a et al., 2018)
Anthocyanins					
Anthocyanin reflectance index	ARI	$\frac{1}{R_{550}} - \frac{1}{R_{710}}$	Fire blight (apple trees), yellow rust (wheat), powdery mildew (wheat)	(Gitelson et al., 2001)	(Devadas et al., 2009; Feng et al., 2016; Skonecny et al., 2020)
Pigments					
Normalized phaeophyte index	NPQI	$\frac{R_{415} - R_{435}}{R_{415} + R_{435}}$	*Xylella fastidiosa* (olive, almond), downy mildew (watermelon)	(Barnes et al., 1992)	(Abdulridha et al., 2022; Camino et al., 2021; Poblete et al., 2020; Zarco-Tejada et al., 2018)
Datt index	DAT	$\frac{R_{672}}{3R_{550}R_{708}}$	*Xylella fastidiosa* (olive, almond)	(Datt, 1998)	(Camino et al., 2021; Poblete et al., 2020; Zarco

					-Tejada et al., 2018)
Blueness index	B	$\frac{R_{450}}{R_{490}}$	Verticillium wilt (olive)	(Zarco-Tejada et al., 2001a)	(Abdulridha et al., 2020; Calderon et al., 2013)
Nitrogen					
Nitrogen reflectance index	NRI	$\frac{R_{570}-R_{670}}{R_{570}+R_{670}}$	Fire blight (apple trees)	(Filella et al., 1995)	(Skoneczny et al., 2020)
Modified chlorophyll absorption in reflectance index at 1510 nm	$MCARI_{1510}$	$\left[\left(R_{700}-R_{1510}\right)-0.2\left(R_{700}-R_{550}\right)\right]\left(\frac{R_{700}}{R_{1510}}\right)$	*Xylella fastidiosa* (almond)	(Haboudane et al., 2002b)	(Camino et al., 2021)
Combined index	CI	$\left(R_{736}-R_{735}\right)\left(R_{850}-R_{720}\right)$ $\left(R_{736}-R_{735}\right)\frac{R_{900}}{R_{720}}$	*Xylella fastidiosa* (almond), *Phytophthora*-induced disease (oak)	(Bao et al., 2013)	(Camino et al., 2021; Hornero et al., 2021)
Ratio spectral index	RSI	$\frac{R_{990}}{R_{720}}$	*Xylella fastidiosa* (almond)	(Yao et al., 2010)	(Camino et al., 2021)
Water content					
Water index	WI	$\frac{R_{900}}{R_{970}}$	Bacterial spot (tomato), target spot (tomato), powdery mildew (wheat)	(Penuelas et al., 1997)	(Abdulridha et al., 2020; Feng

					et al., 2016)
VIs for plant physiological properties					
Xanthophyll and photosynthetic efficiency					
Photochemical reflectance indices and modified forms	PRIs	$PRI = \frac{R_{531} - R_{570}}{R_{531} + R_{570}}$ $\frac{R_{512} - R_{531}}{R_{512} + R_{531}}$ $\frac{R_{570} - R_{531} - R_{670}}{R_{570} + R_{531} + R_{670}}$ $\frac{R_{570} - R_{531}}{R_{570} + R_{531}} / RDVI\left(R_{700} * R_{670}\right)$ $PRI * \left(\frac{R_{900}}{R_{970}} - 1\right)$	Bacterial spot (tomato), target spot (tomato), downy mildew (watermelon), leaf blast (rice), *Xylella fastidiosa* (olive, almond)	(Gamon et al., 1992; Garrity et al., 2011; Zarco-Tejada et al., 2013)	(Abdulridha et al., 2020; Abdulridha et al., 2022; Camino et al., 2021; Poblete et al., 2020; Tian et al., 2021; Zarco-Tejada et al., 2018)
Stresses					
Healthy index	HI	$\frac{R_{534} - R_{698}}{R_{534} + R_{698}} - 0.5R_{704}$	Verticillium wilt (olive), foliar diseases (sugar beet), leaf blast (rice)	(Mahlein et al., 2013)	(Calderon et al., 2013; Mahlein et al., 2013; Tian et al., 2021)

Red-edge vegetation stress index	RVSI	$\frac{R_{714}-R_{752}}{2-R_{733}}$	Powdery mildew (wheat)	(Merton and Huntington, 1999)	(Feng et al., 2016)
Powdery mildew index	PMI	$\frac{R_{520}-R_{584}}{R_{520}+R_{584}}+R_{724}$	Powdery mildew (wheat)	(Mahlein et al., 2013)	(Feng et al., 2016)
Biomass					
Gnyp and Li's index	GnyLi	$\frac{R_{900}R_{1050}-R_{955}R_{1220}}{R_{900}R_{1050}+R_{955}R_{1220}}$	*Phytophthora*-induced disease (oak), *Xylella fastidiosa* (almond)	(Gnyp et al., 2014)	(Camino et al., 2021; Hornero et al., 2021)
Chlorophyll fluorescence					
Lichtenthaler 3	LIC3	$\frac{R_{440}}{R_{740}}$	*Phytophthora*-induced disease (oak)	(Lichtenthaler, 1996)	(Hornero et al., 2021)
Reflectance curvature index	CUR	$\frac{R_{675}R_{690}}{R_{683}^2}$	*Xylella fastidiosa* (almond)	(Zarco-Tejada et al., 2001b)	(Camino et al., 2021)
GPP and phenology					
Reflectance chlorophyll/carotenoid index	CCI	$\frac{R_{531}-R_{645}}{R_{531}+R_{645}}$	Leaf blast (rice)	(Gamon et al., 2016)	(Tian et al., 2021)

Note: Abbr. is an abbreviation for Abbreviation. Similarly, Orig. Ref. is an abbreviation for Original Reference, while Disease Ref. stands for Reference Used for Plant Disease Detection.

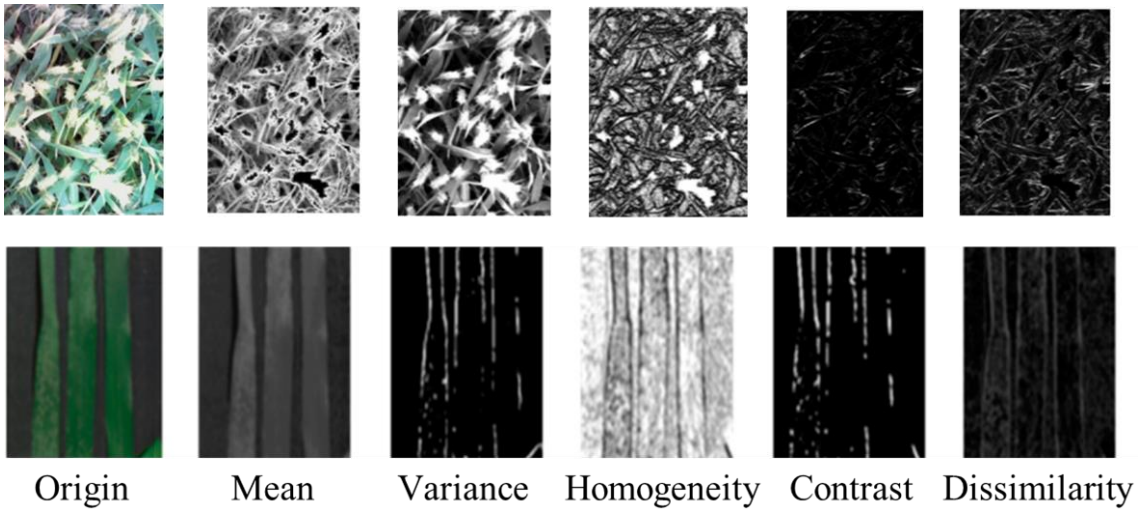

Fig. S2.2. *Five common textural features based on the gray-level co-occurrence matrix (GLCM) at the canopy scale (top row) and foliar scale (bottom row). Top and bottom rows modified from Feng et al. (2022) and Khan et al. (2021), respectively.*

Table S2.2 Overview of key hyperspectral satellite

Satellite	**Launch Purpose**	**Continuous Spectral range (nm)**	**Spectral Resolution (nm)**	**Spatial Resolution (m)**	**Temporal Resolution (days)**	**Launch Date**	**Manufacturer**
EO-1 Hyperion	Environmental monitoring, disaster	357-2576	10	30	16	2000	NASA
PROBA-CHRIS	Land surface characterization	400-1050	34	17	7	2001	ESA
HyspIRI	Ecosystem and disaster monitoring	380-2500	10	60	19	2007	NASA
HJ-1A	Environmental and disaster monitoring	450-950	5	100	4	2008	CNSA
PRISMA	Environmental monitoring, agriculture, resource management	400-2505	≤ 10	30	25	2019	ASI
ENMAP	Environmental mapping and	420-2450	6.5	30	27	2022	DLR
PACE	Ocean color, aerosols, vegetation	340–890	5	1000	1–2+	2024	NASA

References

Abdulridha, J., Ampatzidis, Y., Kakarla, S.C., Roberts, P. (2020). Detection of target spot and bacterial spot diseases in tomato using UAV-based and benchtop-based hyperspectral imaging techniques. *Precision Agriculture, 21*, 955-978

Abdulridha, J., Ampatzidis, Y., Qureshi, J., Roberts, P. (2022). Identification and classification of downy mildew severity stages in watermelon utilizing aerial and ground remote sensing and machine learning. *Frontiers in Plant Science, 13*, 791018

Abdulridha, J., Ehsani, R., de Castro, A. (2016). Detection and differentiation between laurel wilt disease, phytophthora disease, and salinity damage using a hyperspectral sensing technique. *Agriculture, 6*, 56

Bagheri, N., Mohamadi-Monavar, H., Azizi, A., Ghasemi, A. (2018). Detection of Fire Blight disease in pear trees by hyperspectral data. *European Journal of Remote Sensing, 51*, 1-10

Bao, Y., Xu, K., Min, J., Xu, J. (2013). Estimating wheat shoot nitrogen content at vegetative stage from in situ hyperspectral measurements. *Intelligent Automation & Soft Computing, 53*, 2063-2071

Barnes, J.D., Balaguer, L., Manrique, E., Elvira, S., Davison, A.W. (1992). A reappraisal of the use of DMSO for the extraction and determination of chlorophylls a and b in lichens and higher plants. *Environmental and Experimental Botany, 32*, 85-100

Blackburn, G.A. (1998). Spectral indices for estimating photosynthetic pigment concentrations: A test using senescent tree leaves. *International Journal of Remote Sensing, 19*, 657-675

Broge, N.H., Leblanc, E. (2001). Comparing prediction power and stability of broadband and hyperspectral vegetation indices for estimation of green leaf area index and canopy chlorophyll density. *Remote Sensing of Environment, 76*, 156-172

Calderon, R., Navas-Cortes, J.A., Lucena, C., Zarco-Tejada, P.J. (2013). High-resolution airborne hyperspectral and thermal imagery for early, detection of Verticillium wilt of olive using fluorescence, temperature and narrow-band spectral indices. *Remote Sensing of Environment, 139*, 231-245

Camino, C., Calderon, R., Parnell, S., Dierkes, H., Chemin, Y., Roman-Ecija, M., Montes-Borrego, M., Landa, B.B., Navas-Cortes, J.A., Zarco-Tejada, P.J., Beck, P.S.A. (2021). Detection of Xylella fastidiosa in almond orchards by synergic use of an epidemic spread model and remotely sensed plant traits. *Remote Sensing of Environment, 260*, 112420

Chen, J.M. (1996). Evaluation of Vegetation Indices and a Modified Simple Ratio for Boreal Applications. *Canadian Journal of Remote Sensing, 22*, 229-242

Datt, B. (1998). Remote Sensing of Chlorophyll a, Chlorophyll b, Chlorophyll a+b, and Total Carotenoid Content in Eucalyptus Leaves. *Remote Sensing of Environment*

Devadas, R., Lamb, D.W., Simpfendorfer, S., Backhouse, D. (2009). Evaluating ten spectral vegetation indices for identifying rust infection in individual wheat leaves. *Precision Agriculture, 10*, 459-470

Feng, W., Shen, W., He, L., Duan, J., Guo, B., Li, Y., Wang, C., Guo, T. (2016). Improved remote sensing detection of wheat powdery mildew using dual-green vegetation indices. *Precision Agriculture, 17*, 608-627

Feng, Z., Song, L., Duan, J., He, L., Zhang, Y., Wei, Y., Feng, W. (2022). Monitoring wheat powdery mildew based on hyperspectral, thermal infrared, and rgb image data fusion. *Sensors, 22*, 33

Filella, I., Serrano, L., Serra, J., Peñuelas, J. (1995). Evaluating wheat nitrogen status with canopy reflectance indices and discriminant analysis. *Crop Science, 35*, 1400-1405

Gamon, J.A., Huemmrich, K.F., Wong, C.Y.S., Ensminger, I., Garrity, S., Hollinger, D.Y., Noormets, A., Penuelas, J. (2016). A remotely sensed pigment index reveals photosynthetic phenology in evergreen

conifers. *Proceedings of the National Academy of Sciences of the United States of America, 113*, 13087-13092

Gamon, J.A., Peñuelas, J., Field, C.B. (1992). A narrow-waveband spectral index that tracks diurnal changes in photosynthetic efficiency. *Remote Sensing of Environment, 41*, 35-44

Garrity, S.R., Eitel, J.U.H., Vierling, L.A. (2011). Disentangling the relationships between plant pigments and the photochemical reflectance index reveals a new approach for remote estimation of carotenoid content. *Remote Sensing of Environment, 115*, 628-635

Gitelson, A., Keydan, G., Merzlyak, M., Gitelson, C. (2006). Three-band model for noninvasive estimation of chlorophyll carotenoids and anthocyanin contents in higher plant leaves. *Geophysical Research Letters, 33*, L11402

Gitelson, A., Merzlyak, M., Zur, Y., Stark, R., Gritz, U. (2001). Non-destructive and remote sensing techniques for estimation of vegetation status. *Papers in Natural Resources, 1*, 273

Gitelson, A.A., Gritz, Y., Merzlyak, M.N. (2003). Relationships between leaf chlorophyll content and spectral reflectance and algorithms for non-destructive chlorophyll assessment in higher plant leaves. *Journal of Plant Physiology, 160*, 271-282

Gnyp, M.L., Bareth, G., Li, F., Lenz-Wiedemann, V.I.S., Koppe, W., Miao, Y., Hennig, S.D., Jia, L., Laudien, R., Chen, X., Zhang, F. (2014). Development and implementation of a multiscale biomass model using hyperspectral vegetation indices for winter wheat in the North China Plain. *International Journal of Applied Earth Observation and Geoinformation, 33*, 232-242

Gold, K.M., Townsend, P.A., Chlus, A., Herrmann, I., Couture, J.J., Larson, E.R., Gevens, A.J. (2020). Hyperspectral measurements enable pre-symptomatic detection and differentiation of contrasting physiological effects of late blight and early blight in potato. *Remote Sensing, 12*, 286

Haboudane, D., Miller, J.R., Pattey, E., Zarco-Tejada, P.J., Strachan, I.B. (2004). Hyperspectral vegetation indices and novel algorithms for predicting green LAI of crop canopies: Modeling and validation in the context of precision agriculture. *Remote Sensing of Environment, 90*, 337-352

Haboudane, D., Miller, J.R., Tremblay, N., Zarco-Tejada, P.J., Dextraze, L. (2002a). Integrated narrow-band vegetation indices for prediction of crop chlorophyll content for application to precision agriculture. *Remote Sensing of Environment, 81*, 416-426

Haboudane, D., Miller, J.R., Tremblay, N., Zarco-Tejada, P.J., Dextraze, L. (2002b). Integrated narrow-band vegetation indices for prediction of crop chlorophyll content for application to precision agriculture. *Remote Sensing of Environment, 81*, 416-426

Hornero, A., Zarco-Tejada, P.J., Quero, J.L., North, P.R.J., Ruiz-Gomez, F.J., Sanchez-Cuesta, R., Hernandez-Clemente, R. (2021). Modelling hyperspectral- and thermal-based plant traits for the early detection of Phytophthora-induced symptoms in oak decline. *Remote Sensing of Environment, 263*, 112570

Huang, L.-S., Ju, S.-C., Zhao, J.-L., Zhang, D.-Y., Qi, H., Teng, L., Yang, F., Yan, Z. (2015). Hyperspectral measurements for estimating vertical infection of yellow rust on winter wheat plant. *International Journal of Agriculture and Biology, 17*, 1237-1242

Khan, I.H., Liu, H., Li, W., Cao, A., Wang, X., Liu, H., Cheng, T., Tian, Y., Zhu, Y., Cao, W., Yao, X. (2021). Early detection of powdery mildew disease and accurate quantification of its severity using hyperspectral images in wheat. *Remote Sensing, 13*, 3612

Kurihara, J., Koo, V.-C., Guey, C.W., Lee, Y.P., Abidin, H. (2022). Early detection of basal stem rot disease in oil palm tree using unmanned aerial vehicle-based hyperspectral imaging. *Remote Sensing, 14*, 799

Lichtenthaler, H.K. (1996). Vegetation Stress: an Introduction to the Stress Concept in Plants. *Journal of Plant Physiology, 148*, 4-14

Loladze, A., Augusto Rodrigues, F., Jr., Toledo, F., San Vicente, F., Gerard, B., Boddupalli, M.P. (2019). Application of remote sensing for phenotyping tar spot complex resistance in maize. *Frontiers in Plant Science, 10*, 552

Mahlein, A.K., Rumpf, T., Welke, P., Dehne, H.W., Pluemer, L., Steiner, U., Oerke, E.C. (2013). Development of spectral indices for detecting and identifying plant diseases. *Remote Sensing of Environment, 128*, 21-30

Malthus, T.J., Andrieu, B., Danson, F.M., Jaggard, K.W., Steven, M.D. (1993). Candidate high spectral resolution infrared indices for crop cover. *Remote Sensing of Environment, 46*, 204-212

Merton, R., Huntington, J. (1999). Early simulation results of the ARIES-1 satellite sensor for multi-temporal vegetation research derived from AVIRIS. In, *Proceedings of the eighth annual JPL airborne earth science workshop* (pp. 9-11). Pasadena, CA, USA

Penuelas, J., Pinol, J., Ogaya, R., Filella, I. (1997). Estimation of plant water concentration by the reflectance Water Index WI (R900/R970). *International Journal of Remote Sensing, 18*, 2869-2875

Poblete, T., Camino, C., Beck, P.S.A., Hornero, A., Kattenborn, T., Saponari, M., Boscia, D., Navas-Cortes, J.A., Zarco-Tejada, P.J. (2020). Detection of Xylella fastidiosa infection symptoms with airborne multispectral and thermal imagery: Assessing bandset reduction performance from hyperspectral analysis. *ISPRS Journal of Photogrammetry and Remote Sensing, 162*, 27-40

Rouse, J.W., Haas, R.H., Schell, J.A., Deering, D.W. (1974). Monitoring vegetation systems in the Great Plains with ERTS. *NASA Special Publication, 351*, 309

Skoneczny, H., Kubiak, K., Spiralski, M., Kotlarz, J. (2020). Fire blight disease detection for apple trees: hyperspectral analysis of healthy, infected and dry leaves. *Remote Sensing, 12*, 2101

Tian, L., Xue, B., Wang, Z., Li, D., Yao, X., Cao, Q., Zhu, Y., Cao, W., Cheng, T. (2021). Spectroscopic detection of rice leaf blast infection from asymptomatic to mild stages with integrated machine learning and feature selection. *Remote Sensing of Environment, 257*, 112350

Vogelmann, J.E., Rock, B.N., Moss, D.M. (1993). Red edge spectral measurements from sugar maple leaves. *International Journal of Remote Sensing, 14*, 1563-1575

Yao, X., Zhu, Y., Tian, Y., Feng, W., Cao, W. (2010). Exploring hyperspectral bands and estimation indices for leaf nitrogen accumulation in wheat. *International Journal of Applied Earth Observation and Geoinformation, 12*, 89-100

Zarco-Tejada, P.J., Camino, C., Beck, P.S.A., Calderon, R., Hornero, A., Hernandez-Clemente, R., Kattenborn, T., Montes-Borrego, M., Susca, L., Morelli, M., Gonzalez-Dugo, V., North, P.R.J., Landa, B.B., Boscia, D., Saponari, M., Navas-Cortes, J.A. (2018). Previsual symptoms of Xylella fastidiosa infection revealed in spectral plant-trait alterations. *Nature Plants, 4*, 432-439

Zarco-Tejada, P.J., González-Dugo, V., Williams, L.E., Suárez, L., Berni, J.A.J., Goldhamer, D., Fereres, E. (2013). A PRI-based water stress index combining structural and chlorophyll effects: Assessment using diurnal narrow-band airborne imagery and the CWSI thermal index. *Remote Sensing of Environment, 138*, 38-50

Zarco-Tejada, P.J., Miller, J.R., Mohammed, G.H., Noland, T.L., Sampson, P.H. (2001a). Estimation of chlorophyll fluorescence under natural illumination from hyperspectral data. *International Journal of Applied Earth Observation and Geoinformation, 3*, 321-327

Zarco-Tejada, P.J., Miller, J.R., Noland, T.L., Mohammed, G.H., Sampson, P.H. (2001b). Scaling-up and model inversion methods with narrow-band optical indices for chlorophyll content estimation in closed

forest canopies with hyperspectral data. *IEEE Transactions on Geoscience and Remote Sensing, 39*, 1491-1507